Journal of Nuclear Materials 463 (2015) 889–892

Contents lists available at ScienceDirect

Journal of Nuclear Materials

journal homepage: www.elsevier.com/locate/jnucmat

Scrape-off layer ion temperature measurements at the divertor target during type III ELMs in MAST measured by RFEA

S. Elmore [a,*], S.Y. Allan [a], G. Fishpool [a], A. Kirk [a], M. Kočan [b], P. Tamain [c], A.J. Thornton [a], the MAST Team [a]

[a] CCFE, Culham Science Centre, Abingdon, Oxon OX14 3DB, UK
[b] ITER Organization, Route de Vinon sur Verdon, 13115 St Paul-lez-Durance, France
[c] Association Euratom-CEA, CEA/DSM/IRFM, CEA-Cadarache, F-13108 St Paul-lez-Durance Cedex, France

ARTICLE INFO

Article history:
Available online 28 September 2014

ABSTRACT

Edge-localised modes (ELMs) can carry significant fractions of their energy as far as main chamber plasma-facing components in divertor tokamaks. Since in future devices (e.g. ITER, DEMO) these energies could cause issues for material lifetime and impurity production, the energy and temperature of ions in ELMs needs to be investigated. In MAST, novel divertor measurements of T_i during ELMs have been made using the divertor retarding field energy analyser (RFEA) probe. These measurements have shown instantaneous ion energy distributions corresponding to an effective T_i at 5 cm from the strike point at the target that can be as high as 60 eV and that this decreases with time after the ELM start. This is consistent with the hottest, fastest ions arriving at the target first by parallel transport, followed by the lower end of the ion energy distribution. This analysis will form a basis for future data analysis of fast swept measurements of ion distributions in ELMs.

1. Introduction

Measurements in JET have shown edge-localised modes (ELMs) to carry significant fractions of their energy to first wall materials [1]. This could be a dominant source of thermal loading and impurity sputtering in future devices such as ITER and DEMO [2]. Measurements of the ion temperature (T_i) and energy have been attempted in a number of present tokamaks such as JET [1], ASDEX-Upgrade [2,3] and MAST [4] at the midplane using retarding field energy analyser (RFEA) probes, however, previously no measurements have been made at the divertor target in a tokamak. Using the divertor RFEA installed in MAST in 2012 [5], the ion energy distribution can be investigated at the outer divertor of MAST during ELM events. Two different measurement techniques have been attempted; a slow-swept method which can give information about the average ELM at a fixed point relative to the divertor strike point, as used in AUG [3]; and a fast-swept method which attempts to analyse the ion distribution on timescales shorter than the time taken for all ions in an ELM to arrive at the divertor. The fast swept measurements, although interesting and novel, prove to be more challenging to analyse due to capacitive effects in the probe which are comparable to the current signal measured.

In this paper the slow swept data will be studied in detail in an attempt to interrogate the time history of ions arriving at the outer divertor as a result of type-III ELM events. These type of ELMs are less dangerous than type-I ELMs, which were previously measured in JET [1], and have a higher frequency which higher statistical measurements. An average ion temperature can be determined from the slow swept data for a set of similar ELMs at a fixed position relative to the strike point. Further information of the time history of the ion energies can be determined by 'box-carring' the signals in 50 μs time intervals, provided the signals from the ELMs are aligned in time.

2. Experimental setup

Ion temperature measurements were made at the outer divertor target of MAST during ELMs using the divertor RFEA probe [5]. Measurements of type III ELMs resulting from a double null plasma with plasma current of $I_p = 600$ kA and neutral beam heating power of $P_{NBI} = 1.8$ MW were made during ELMy H-mode periods, during which the position of the strike point relative to the divertor RFEA was fixed at two radial positions, accurate to ±0.5 cm from infra-red (IR) measurements.

The RFEA is operated in the slow swept mode, where it is assumed that during the lifetime of an ELM event, the voltage on the discriminating grid (grid 1) is approximately constant. The voltage is swept from 0 V to ~300 V at 40 Hz. This is similar to

* Corresponding author at: EURATOM/CCFE Fusion Association, Culham Science Centre, Abingdon, Oxon OX14 3DB, UK.
E-mail address: Sarah.Elmore@ccfe.ac.uk (S. Elmore).

http://dx.doi.org/10.1016/j.jnucmat.2014.09.039
0022-3115/

the method used in the AUG RFEA ELM measurements [2,3]. The slit plate was held at a constant voltage of −200 V in order to repel electrons and measure the saturation current density, j_{sat}. Grid 2, used for suppression of secondary electrons, was held at a constant voltage of −300 V. See Fig. 1 for a diagram of the RFEA setup. The effective temperature of the ion energy distribution during an ELM can be determined by comparing the slit plate and collector currents during ELMs at various grid 1 voltages. The average collector current during an ELM is defined as [3]:

$$\langle I_c \rangle_{ELM} = \Delta t_{ELM}^{-1} \int_{\Delta t_{ELM}} I_c \, dt \tag{1}$$

where Δt_{ELM} is the duration of the ELM signal, defined by the time that j_{sat} on the RFEA slit plate is greater than $0.1 * \left(j_{sat}^{peak\ ELM} - j_{sat}^{inter-ELM}\right) + j_{sat}^{inter-ELM}$, and I_c is the measured current at the collector plate.

It is assumed that during the measurements, ELM events enhance the steady state plasma at the RFEA probe and therefore the measurements are a combination of inter-ELM and ELM ions. In order to calculate T_i for purely the ELM ions, the steady state ion current arriving at the collector plate due to the scrape-off layer (SOL) plasma has been removed before $\langle I_c \rangle_{ELM}$ is calculated. The background ion current, I_{BKGD}, of ions resulting from steady state SOL plasma can be estimated for the specific radial location of the measurements using steady state data obtained in the same plasma scenario [6]. Using the measured inter-ELM T_e, T_i and j_{sat} profiles, I_{BKGD} can be determined for a particular distance of from the strike point at the target (ΔR_{LCFS}^{tgt}) using an assumed transmission through the probe, $T_r \sim A_s \xi_r \xi_{opt}^3$, where A_s is the slit area, ξ_r is the estimated transmission through the probe slit, and ξ_{opt} is the optical transmission through the grids. Using the following steady state equation I_{BKGD} can be calculated for the particular constant applied grid voltage (V_g) during the ELM.

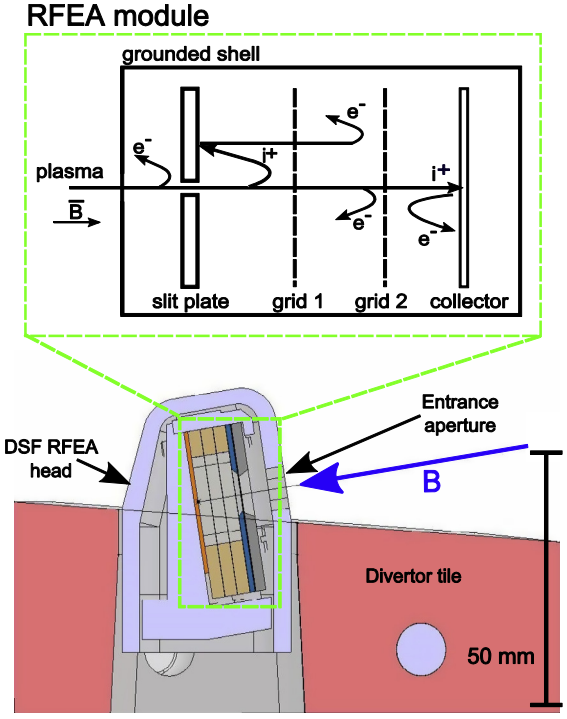

Fig. 1. Schematic of RFEA module in operation and cross-section of divertor RFEA in the MAST lower outer divertor target.

$$I_{BKGD} = A_s \xi_r \xi_{opt}^3, \quad V_g < 2.7T_e$$
$$I_{BKGD} = A_s \xi_r \xi_{opt}^3 j_{sat} \exp\left(\frac{-(V_g - 2.7T_e)}{T_i}\right), \quad V_g \geqslant 2.7T_e \tag{2}$$

I_{BKGD} is subtracted from I_c to give I_{cELM} before integrating using Eq. (1). For the radius ranges used in this analysis inter-ELM T_i = 13.5–16 eV, T_e = 7.5–8 eV and j_{sat} = 0.7–1.3 kA m^{-2}.

To remove any biasing effect on the collector measurements resulting from variation in the flux across ELM events, the collector current, I_c for an ELM is normalised to j_{sat}. The time averaged j_{sat}, $\langle j_{sat} \rangle_{ELM}$, is calculated in the same way as Eq. (1). By comparing the ratio of the slit plate and collector currents for a set of similar ELMs at a fixed ΔR_{LCFS}^{tgt}, T_i can be determined using the following:

$$\frac{\langle I_c \rangle_{ELM}}{\langle j_{sat} \rangle_{ELM}} = T_r \exp\left(\frac{-(V_g - V_s)}{T_i}\right) + C \tag{3}$$

T_r can be estimated from probe dimensions. However in this analysis it will be a fitted parameter along with V_s, the sheath voltage, which is defined as $V_s = 2.7T_e$ [3], T_i, and C, which accounts for any offsets in the current signals.

It is possible to interrogate the evolution of the ion distribution arriving at the divertor RFEA in time by analysing separate time cuts through Δt_{ELM} rather than calculating T_i for the time-averaged ELM. First the ELMs must be aligned in time so that the time windows analysed are comparable for all ELMs. The alignment is done by finding the leading edge of the ELMs on the slit plate j_{sat} signal. The leading edge is defined as the point at which j_{sat} signal reaches $0.5 * \left(j_{sat}^{peakELM} + j_{sat}^{inter-ELM}\right)$; this time is labelled t_{ELM}. Once all ELMs at a fixed ΔR_{LCFS}^{tgt} are aligned, the currents are divided into 50 μs windows starting at t_{ELM} until t_{ELM} + 300 μs, see Fig. 2 for an example j_{sat} signal with time window cuts shown. These windows become Δt_{ELM} in Eq. (1) and the ratio of $\langle I_c \rangle_{ELM} / \langle j_{sat} \rangle_{ELM}$ as a function of t–t_{ELM} from t_{ELM} to t_{ELM} + 300 μs can be constructed. This allows, for each 50 μs time window, the normalised current ratio to be plotted against grid 1 voltage for the set of ELMs and therefore T_i, V_s and t_0 to be determined as a function of t–t_{ELM}.

3. ELM T_i measurements

A set of similar type III ELMs have been measured at $\Delta R_{LCFS}^{tgt} \sim 5$ cm and $\Delta R_{LCFS}^{tgt} \sim 7$ cm, where $\lambda_q^{tgt} \sim 3$ cm as measured

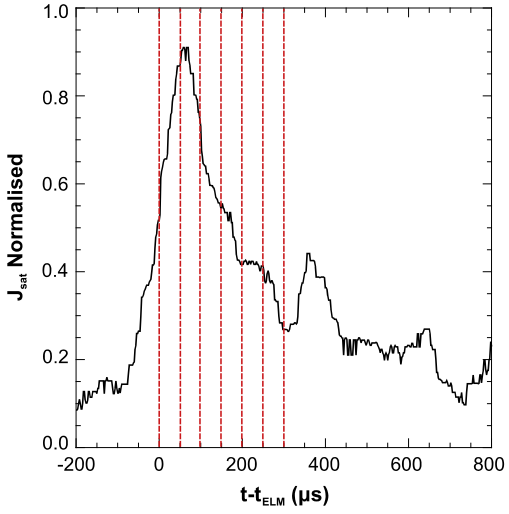

Fig. 2. Typical normalised j_{sat} signal during an ELM, aligned to t_{ELM}. Red lines indicate cuts in time used for boxcar time dependant analysis. All time intervals are Δt_{ELM} = 50 μs. (For interpretation of the references to colour in this figure legend, the reader is referred to the web version of this article.)

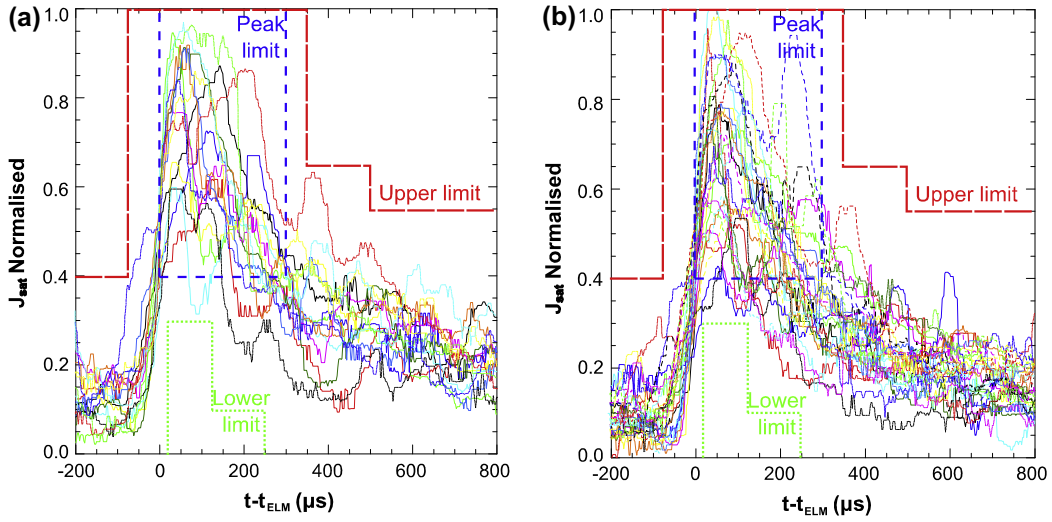

Fig. 3. Set of similar ELMs which fit within the constrained window for (a) $\Delta R^{tgt}_{LCFS} \sim 5$ cm and (b) $\Delta R^{tgt}_{LCFS} \sim 7$ cm. Red dotted lines display the upper limit on normalized j_{sat}; green dotted lines display the lower limit on j_{sat}; and blue dotted lines require that maximum peaks are above a minimum fraction of the largest ELM and occur within a range of time following the time defined as t_{ELM}. (For interpretation of the references to colour in this figure legend, the reader is referred to the web version of this article.)

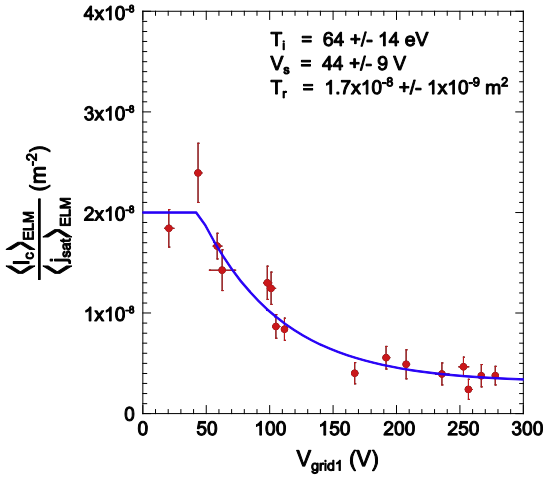

Fig. 4. Example fitted characteristic of $\langle I_c\rangle_{ELM}/\langle j_{sat}\rangle_{ELM}$ vs V_g for $t_{ELM} < t < t_{ELM} + 50$ μs at $\Delta R^{tgt}_{LCFS} \sim 5$ cm.

by IR. Similar ELMs to be analysed as a set have been determined by requiring the j_{sat} signals, normalised to the largest peak signal, to fit within a pre-determined shape of the rise and fall as a function of time. Fig. 3 shows the chosen ELMs for each radial position, where the red dotted lines display the upper limit on normalised j_{sat}; the green dotted lines display the lower limit on j_{sat}; and the blue dotted lines require that maximum peaks are above a minimum fraction of the largest ELM and that they occur within a range of time following the time defined as t_{ELM}. If it is assumed that any variations in the j_{sat} signal with time are caused by changes in density and not in temperature, then determining the inferred T_i using the ratio of $\langle I_c\rangle_{ELM}$ to $\langle j_{sat}\rangle_{ELM}$ will remove any effects due to j_{sat} magnitude variations.

For each 50 μs time window the ratio of integrated currents, $\langle I_c\rangle_{ELM}/\langle j_{sat}\rangle_{ELM}$, is plotted against voltage, V_g, and using Eq. (2), T_i, V_s and T_r can be determined; see Fig. 4 for a characteristic for the time window 0 μs > t_{ELM} > 50 μs, at $\Delta R^{tgt}_{LCFS} \sim 5$ cm.

Using the fitted parameters from the characteristics, T_i, V_s and T_r can be plotted as a function of time through the 'average' type III ELM in this particular MAST plasma scenario, see Fig. 5, measured at $\Delta R^{tgt}_{LCFS} \sim 5$ cm and $\Delta R^{tgt}_{LCFS} \sim 7$ cm. Peak T_i is measured at t_{ELM}, where t_{ELM} is half the time of the rise on j_{sat}, of $T_i \sim 64$ eV at $\Delta R^{tgt}_{LCFS} \sim 5$ cm and $T_i \sim 27$ eV at $\Delta R^{tgt}_{LCFS} \sim 7$ cm. Fig. 5 shows T_i reduces with time after the ELM start, t_{ELM}, with the hottest ions measured closest to the divertor strike point for t–t_{ELM} < 100 μs. Both sets of ELMs show a similar reduced T_i after t–$t_{ELM} \sim 100$ μs. This suggests that most hot ions arrive at the target before t_{ELM} + 100 μs, which is consistent with estimated parallel transport times for ELM ions. The difference in T_i for the two measurement

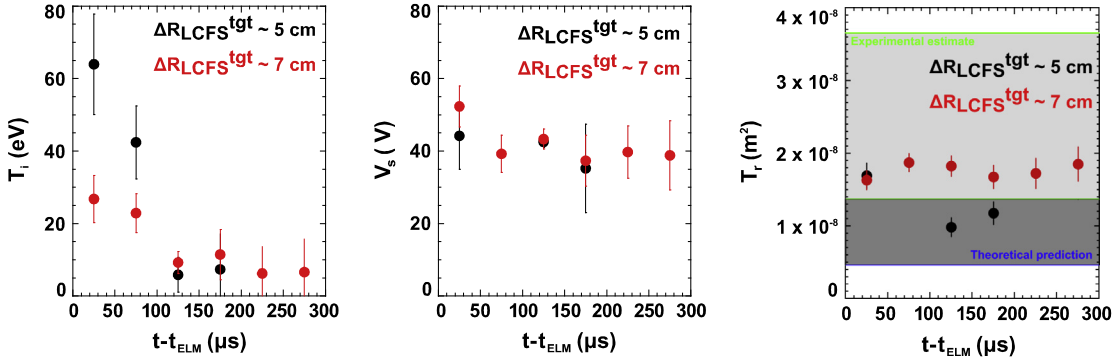

Fig. 5. Time dependant results of T_i, V_s and T_r for similar type III ELMs at $\Delta R^{tgt}_{LCFS} \sim 5$ cm and $\Delta R^{tgt}_{LCFS} \sim 7$ cm. Also shown are the theoretical prediction and the experimental estimate of t_0 for the MAST divertor RFEA.

positions also suggests less hot ions reach the divertor target at larger distances from the strike point and although temperatures ~60 eV are measured at $\Delta R^{tgt}_{LCFS} \sim 5$ cm, these reduce considerably a few cm further from the strike point.

V_s, which is proportional to T_e, shows a slight initial peak at t_{ELM}. Since $V_s \sim 2.7T_e$, we measure $T_i \sim 3.8T_e$ at t_{ELM} at $\Delta R^{tgt}_{LCFS} \sim 5$ cm and $T_i \sim 1.5T_e$ at t_{ELM} at $\Delta R^{tgt}_{LCFS} \sim 7$ cm. This shows a reduction in both T_i and T_i/T_e with distance from the strike point at the target. V_s has a slight tendency to reduce after t_{ELM}, and settles at a relatively constant value for both radial positions of $V_s \sim 40$ V at ΔR^{tgt}_{LCFS} over the following 300 μs.

It can be seen that T_r remains relatively constant, on average, as would be expected, since it is largely determined by the geometry of the RFEA probe. The values estimated from the fitted data correspond to $\xi_r \sim 0.2$–0.4; which spans the range of estimated values calculated from Kočan's model [7] using the dimensions of the MAST divertor RFEA probe; $\xi_r \sim 0.2$–0.3. It is expected that value of ξ_r could be larger than those theoretically calculated since the attenuation of the MAST RFEA protective housing could mean the theoretical current transmitted is an underestimation. Values for ξ_r estimated experimentally from the divertor RFEA probe on MAST [5] show values in the range $\xi_r \sim 0.3$–0.8, therefore incorporating the transmission estimated here from the fitted characteristics.

4. Summary

Slow swept data analysis of type III ELMs has been exploited to gain understanding of the evolution of T_i and V_s through an ELM arriving at the target. This information will provide a basis for which to compare fast swept RFEA ELM data to be analysed in the near future. Both T_i and V_s are seen to reduce through time which is consistent with the model of hot ions draining from the ELM faster than the cooler ions. It has also been shown that at larger ΔR^{tgt}_{LCFS}, T_i^{ELM} reduces; consistent with hot ions being lost at smaller R. The transmission through the probe is consistent with that expected from theoretical predictions for the dimensions of the MAST divertor RFEA. Further analysis will tackle type I and type III ELMs measured by the fast swept method, for which this work will allow valuable comparison. Future kinetic modelling will be used along with these measurements in order to investigate the loss process in ELMs.

Acknowledgements

This work was part-funded by the RCUK Energy Programme [Grant Number EP/I501045] and by the European Union's Horizon 2020 research and innovation programme. To obtain further information on the data and models underlying this paper please contact PublicationsManager@ccfe.ac.uk. The views and opinions expressed herein do not necessarily reflect those of the European Commission.

References

[1] R.A. Pitts et al., Nucl. Fusion 46 (2006) 82–98.
[2] M. Kočan et al., Nucl. Fusion 52 (2012) 023016.
[3] M. Kočan et al., Plasma Phys. Control Fusion 53 (2011) 065002.
[4] P. Tamain et al., J. Nucl. Mater. 415 (2011) S1139–S1142.
[5] S. Elmore et al., Plasma Phys. Control Fusion 54 (2012) 065001.
[6] S. Elmore et al., J. Nucl. Mater. 438 (2013) S1212–S1215.
[7] M. Kočan et al., Rev. Sci. Instrum. 79 (2008) 073502.